Supplementary Information

Unravelling relativistic fermions in Weyl semimetal TaAs by magnetostriction measurements

Tomasz Cichorek, Łukasz Bochenek, and Jarosław Juraszek

Institute of Low Temperature and Structure Research, Polish Academy of Sciences, 50-422 Wrocław, Poland

Yuriy V. Sharlai and Grigorii P. Mikitik

B. Verkin Institute for Low Temperature Physics and Engineering, Ukrainian Academy of Sciences, Kharkov 61103, Ukraine

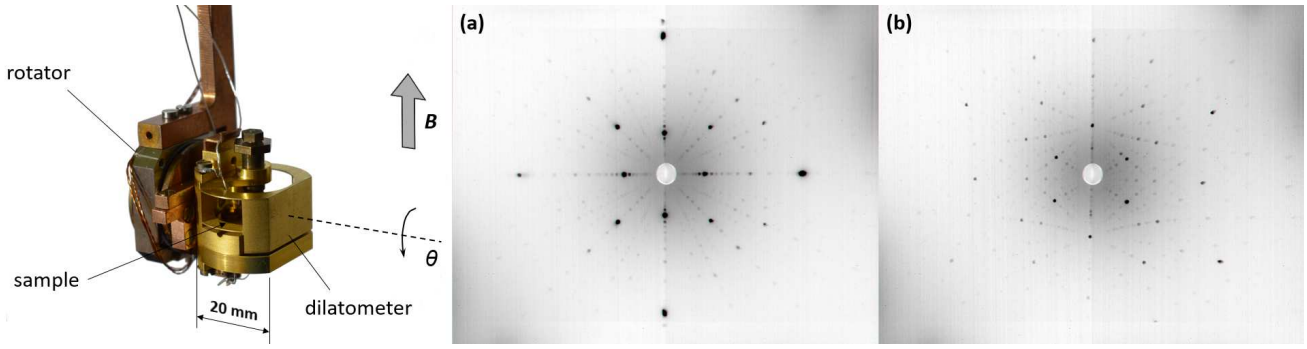

Supplementary Fig. 1. Left: Photograph of the commercial dilatometer cell [1] mounted on a cold finger of a dilution refrigerator. This setup is equipped with a piezoelectric rotator for angle-dependent magnetostriction. Right: Back-reflection Laue photographs of the TaAs single crystal (sample 1). Figure (a) shows the diffractogram along the c axis, whereas (b) shows the diffractogram along the a axis.

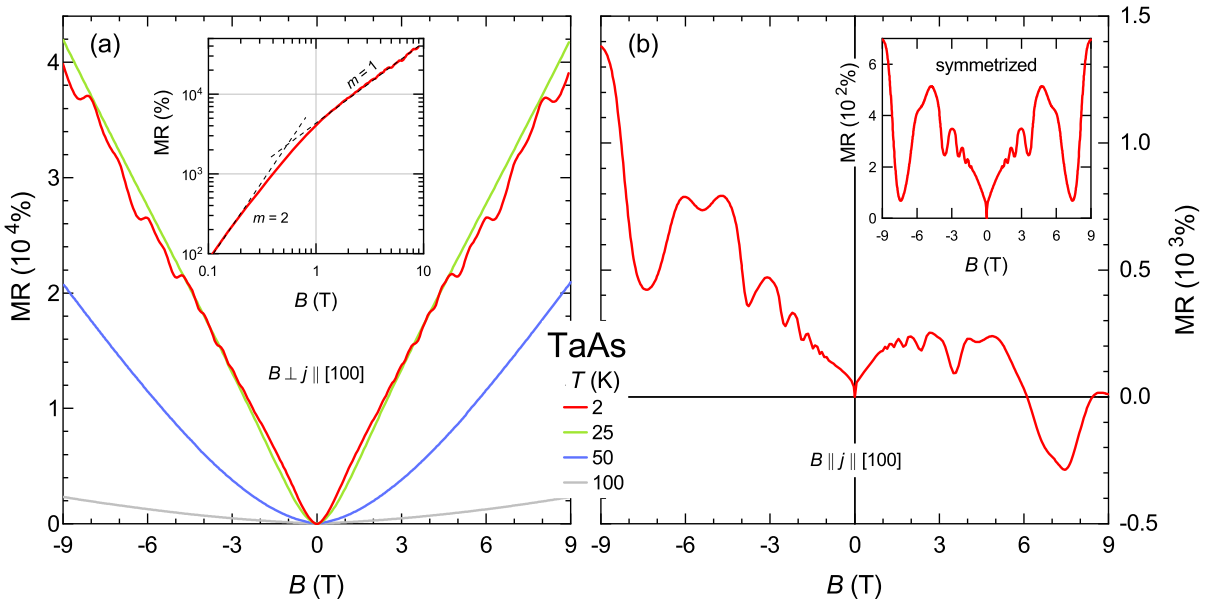

Supplementary Fig. 2. Transverse (a) and longitudinal (b) magnetoresistance of TaAs measured along the a axis. No off-diagonal components were subtracted from the MR data shown in main panels.

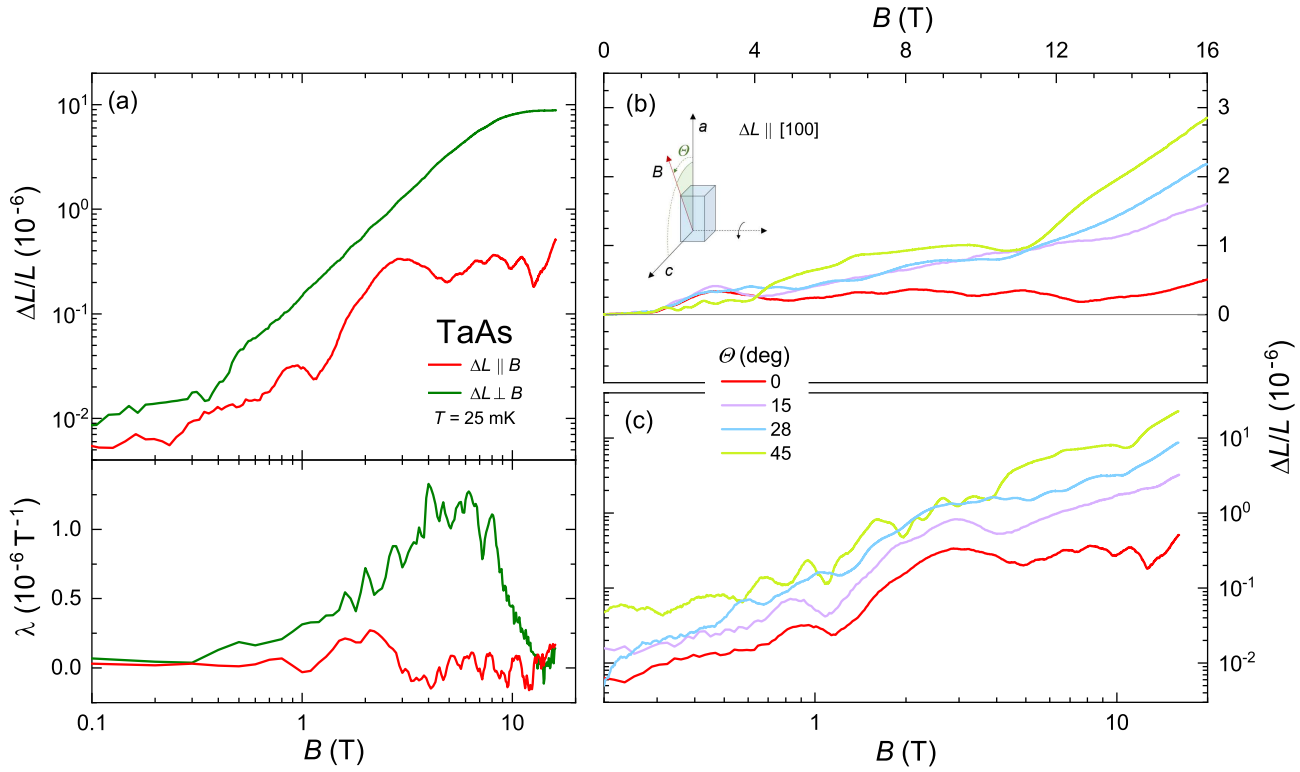

Supplementary Fig. 3. The a-axis magnetostriction of TaAs measured within the (010) plane at 25 mK. (a) Top: Magnetic-field dependence of the relative length change $\Delta L/L$ measured along the [100] direction both in the parallel (red) and perpendicular (green) configuration. At 16 T, the $\Delta L \parallel B$ and $\Delta L \perp B$ data differ by more than one order of magnitude. Bottom: Magnetostriction coefficient λ derived from the longitudinal and transverse measurements. (b) Complex dependences of the magnetostriction at small tilt angles $\Theta \leq 45°$. Note a small longitudinal magnetostriction in the entire field range (red). (c) Log-log plot of the experiential results shown in (b). Curves are subsequently shifted by a factor of 3 for clarity.

Supplementary Note 1: Formula for the magnetostriction

We now derive the general formula for the magnetostriction [formula (1) in the main text], assuming, for definiteness, the tetragonal symmetry of a crystal (i.e., the symmetry of TaAs). This formula can be obtained by a minimization of the Ω potential for the deformed crystal placed in the external magnetic field H with respect to the strain tensor u_{ik},

$$\begin{aligned}\Omega = &\frac{1}{2}C_{11}(u_{xx}^2+u_{yy}^2)+\frac{1}{2}C_{33}u_{zz}^2\\ &+C_{13}(u_{xx}+u_{yy})u_{zz}+C_{12}u_{xx}u_{yy}\\ &+2C_{66}u_{xy}^2+2C_{44}(u_{xz}^2+u_{yz}^2)\\ &+\Delta\Omega_{\rm el}(u_{ik},B)-\Delta\Omega_{\rm el}(u_{ik},0),\end{aligned} \tag{1}$$

where C_{mn} are the elastic moduli of the crystal [2], $B=\mu_0 H$ is the magnetic induction in the sample, $\Delta\Omega_{\rm el}(u_{kl},B)\equiv\Omega_{\rm el}(u_{kl},B)-\Omega_{\rm el}(0,B)$, and $\Omega_{\rm el}(u_{kl},B)=\sum_{i=1}^{N}\Omega_i(u_{kl},B)$ is the electron part of the Ω potential for the crystal with N pockets of charge carriers. This part depends on the deformation, the magnetic induction B, and also on the temperature T and the chemical potential ζ (we do not indicate explicitly T and ζ here). The first six terms in Eq. (1) give the total elastic energy of a deformation. This energy is partly produced by $\Delta\Omega_{\rm el}(u_{kl},0)$, and hence the difference of the elastic terms and $\Delta\Omega_{\rm el}(u_{kl},0)$ is the elastic energy that is not associated with the electron pockets under study. The term $\Delta\Omega_{\rm el}(u_{kl},B)$ describes the total change in the Ω potential of these pockets in the magnetic field under the deformation. As in Ref. [3–6], we assume that an elastic deformation shifts the electron bands as a whole and does not change their shape. This rigid-band approximation commonly is well justified for sufficiently small pockets. In particular, this approximation seems to be valid for TaAs family of the semimetals, see Figs. 6e and 6f in Ref. [7]. In this rigid-band approximation, a shift $\Delta\varepsilon_i$ of the ith electron energy band $\varepsilon_i(\mathbf{p})$ under the deformation coincides with the shift of its edge and is proportional to the strain tensor u_{kl}, $\Delta\varepsilon_i=\sum_{k,l}\lambda_{kl}^{(i)}u_{kl}$, where the constants $\lambda_{kl}^{(i)}$ are the so-called deformation potential of the ith band [8]. Therefore, in the minimization of Ω potential, one can use the following relation:

$$\frac{\partial\Omega_i(u_{kl},B)}{\partial u_{kl}}=-\frac{\partial\Omega_i(\zeta,B)}{\partial\zeta}\frac{\partial\Delta\varepsilon_i}{\partial u_{kl}}=\lambda_{kl}n_i(B),$$

where $n_i(B)=-\partial\Omega_i(\zeta,B)/\partial\zeta$ is the density of charge carriers of the pocket i in the magnetic field. The minimization gives a set equations in u_{kl}, which define the magnetostriction, i.e., the deformation of the crystal in the magnetic field. Solving this set of the equations, we specifically obtain,

$$u_{zz}=\sum_i^N\Lambda_i[n_i(B)-n_i(0)], \tag{2}$$

$$\Lambda_i=-\frac{\lambda_{zz}^{(i)}(C_{11}+C_{12})-2C_{13}\lambda_{xx}^{(i)}}{C_{33}(C_{11}+C_{12})-2(C_{13})^2}. \tag{3}$$

The same formula (2) describes u_{xx} and u_{yy} but with the other Λ_i,

$$\Lambda_i=-\frac{\lambda_{xx}^{(i)}C_{33}-\lambda_{zz}^{(i)}C_{13}}{C_{33}(C_{11}+C_{12})-2(C_{13})^2}. \tag{4}$$

The u_{zz} is the elongation $\Delta L/L$ of the crystal along the direction [001], whereas u_{xx} is the elongation in the direction [100]. Formulas (3) and (4) show that the constants Λ_i extracted from the measurements of u_{zz} and u_{xx} enable one to find the constants $\lambda_{zz}^{(i)}$, $\lambda_{xx}^{(i)}$ of the deformation potential if the the elastic moduli C_{mn} are known. (In particular, these moduli for TaAs are given in Ref. [9].)

For definiteness, we shall discuss only u_{zz} below. Note that formula (2) was used in Refs. [4–6]. (In the paper [6] corrections to Eq. (2) were also taken into account when the chemical potential is close to the edge of a Landau subband.)

Supplementary Note 2: Magnetostriction produced by Weyl electrons in noncentrosymmetric crystals

As was shown in Sec. 3.3 of Ref. [10], for a *noncentrosymmetric* crystal, a contribution of a Fermi pocket of Weyl quasiparticles to any thermodynamic quantity (including the magnetostriction) can be calculated as half of the appropriate contribution of the Dirac pocket with the same electron dispersion. Using formulas for the electron spectrum in the magnetic field in the vicinity of a Dirac point [10, 11], the Ω potential and hence the density $n(B)$ of the Weyl electrons can be found. In particular, we obtain at zero temperature,

$$n(\zeta-\varepsilon_d,B)=n(\zeta-\varepsilon_d,0)\Big(\frac{3}{4u}+\frac{3}{2u^{3/2}}\sum_{n=1}^{n=[u]}\sqrt{u-n}\Big), \tag{5}$$

where $n(\zeta-\varepsilon_d,B)$ is the density of the Weyl quasiparticles in the magnetic field $H=B/\mu_0$ at a given chemical potential ζ; the density in absence of the magnetic field, $n(\zeta-\varepsilon_d,0)$, is assumed to be positive in the case of the electrons ($\zeta-\varepsilon_d>0$) and negative for the holes ($\zeta-\varepsilon_d<0$); ε_d is the energy of the Weyl point; $[u]$ means the integer part of $u\equiv F/B$; the frequency of the quantum oscillations

$$F=\frac{S_{\max}}{2\pi e\hbar} \tag{6}$$

also defines the boundary of the ultra-quantum region at which these oscillations disappear, and $S_{\max}$ is the maximal cross sectional area of the Fermi surface of the Weyl

quasiparticles at a given direction of the magnetic field. This area is proportional to $(\zeta-\varepsilon_d)^2$. Of course, formula (5) is applicable to the case of the Dirac electrons, too. We also point out the two useful representations of the sum in Eq. (5),

$$\sum_{n=1}^{n=[u]}\sqrt{u-n}=\zeta(-1/2,\{u\})-\zeta(-1/2,u), \qquad (7)$$

$$\sum_{n=1}^{n=[u]}\sqrt{u-n}=-\mathrm{Im}\{\zeta(-1/2,1-u-0i)\}, \qquad (8)$$

where $\zeta(-1/2,u)$ is the Hurwitz zeta function [12], and $\{u\}\equiv u-[u]$ is the fractional part of u.

We emphasize that formula (5) is valid for the most general form of the dispersion laws $\varepsilon_c(\mathbf{p})$ and $\varepsilon_v(\mathbf{p})$ describing the quasiparticles in the vicinity of the Weyl point [10],

$$\varepsilon_{c,v}(\mathbf{p})=\varepsilon_d+\mathbf{a}\cdot\mathbf{p}\pm E(\mathbf{p}),$$
$$E(\mathbf{p})=[b_{11}p_1^2+b_{22}p_2^2+b_{33}p_3^2]^{1/2},$$

where $\mathbf{a}=(a_1,a_2,a_3)$ and b_{ii} are the constant parameters, with a_i specifying the so-called tilt of the spectrum. For reference, let us also write the expressions for $n(\zeta-\varepsilon_d,0)$ and $S_{\max}$ in terms of these parameters,

$$n(\zeta-\varepsilon_d,0)=\frac{(\zeta-\varepsilon_d)^3}{3\pi^2\hbar^3(b_{11}b_{22}b_{33})^{1/2}(1-\tilde{a}^2)^2},$$
$$S_{\max}=\frac{\pi(\zeta-\varepsilon_d)^2}{(1-\tilde{a}^2)R_n^{1/2}},$$

where $\tilde{a}^2\equiv\tilde{a}_1^2+\tilde{a}_2^2+\tilde{a}_3^2$, $\tilde{a}_i\equiv a_i/\sqrt{b_{ii}}$,

$$R_n=\sum_{i,j=1}^{3}\kappa^{ij}n_in_j$$
$$\kappa^{ij}=\frac{b_{11}b_{22}b_{33}}{(b_{ii}b_{jj})^{1/2}}\left[(1-\tilde{a}^2)\delta_{ij}+\tilde{a}_i\tilde{a}_j\right],$$

δ_{ij} is the Kronecker symbol, and $\mathbf{n}=(n_1,n_2,n_3)$ is the unit vector along the magnetic field.

Formulas (2) and (5) describe the magnetostriction u_{zz} produced by the Weyl electrons at zero temperature T and in absence of the electron scattering by impurities. It was demonstrated by Shoenberg [13] that the effect of the impurities on the oscillating part of the magnetization can be taken into account by replacing the Fermi energy E_F (i.e. ζ at $T=0$) by $E_F+i\Gamma$ where the parameter $\Gamma=\pi T_D$ characterizes the electron scattering by the impurities, and T_D is the so-call Dingle temperature. We shall use this replacement both for the oscillating and for the smooth parts of the magnetostriction. In other words, to take into account the scattering, the parameter $u+0i$ in formula (8) is replaced by $u(1+i\gamma)^2$ where $\gamma\equiv\Gamma/(\zeta-\varepsilon_d)=\pi t_D$ is the dimensionless characteristic of the scattering, and t_D is the dimensionless Dingle

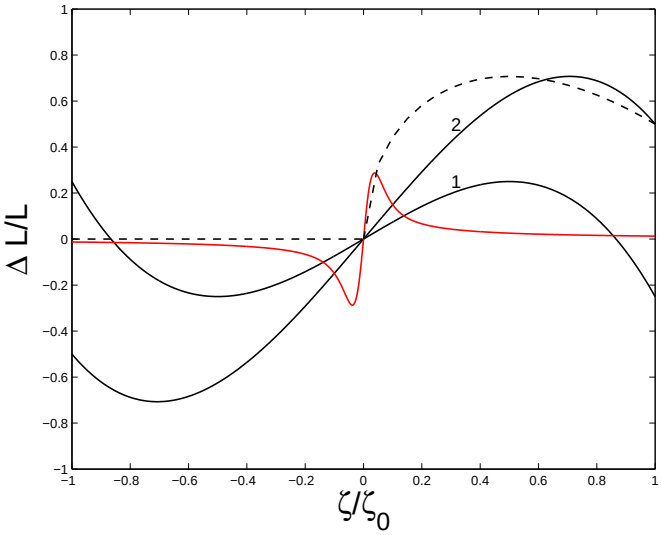

Supplementary Fig. 4. The magnetostriction $\Delta L/L=u_{zz}$ (in units of $\Lambda n(\zeta_0,0)$) produced by the Weyl electrons at $T=0$ versus the dimensionless chemical potential ζ/ζ_0 for $\mu_0H/F=2$ and $\mu_0H/F=1$ (the black solid lines, the numbers near these lines indicate the values of μ_0H/F). The chemical potential ζ is measured from the ε_d, and ζ_0 is its initial value. The solid red line shows the smooth part of the magnetostriction, $\bar{u}_{zz}$, enlarged in 10 times for $\mu_0H/F=1/7$ and for the nonzero temperature $T/\zeta_0=0.02$. The dashed line depicts the dependence of the magnetostriction on the chemical potential ζ at $T=0$, $\mu_0H/F=2$ for the crystal with the electron spectrum (17) and $\delta=1/2$ (the chemical potential is now measured from ε_0). Note that this dependence, which vanishes below ε_0, qualitatively differs from the dependence for the Weyl electrons.

temperature. As to the magnetostriction at $T>0$, it can be obtained as follows:

$$u_{zz}(\zeta,T,H)=\int_{-\infty}^{\infty}d\varepsilon\frac{u_{zz}(\varepsilon,0,H)}{4T\cosh^2[(\varepsilon-\zeta)/2T]}. \qquad (9)$$

Consider now various limiting cases.

Ultra-quantum regime ($\mu_0H>F$). At high fields $\mu_0H>F$, the sum in equation (5) disappears since $u=F/B<1$ in this case. Then, with formula (2), we obtain the following contribution of a Weyl pocket to the magnetostriction:

$$u_{zz}=\Lambda n(\zeta-\varepsilon_d,0)\left(\frac{3B}{4F}-1\right)\equiv a+bB, \qquad (10)$$

where the quantities Λ, $n(\zeta-\varepsilon_d,0)$, F introduced above and $a\equiv-\Lambda n(\zeta-\varepsilon_d,0)$, $b\equiv-0.75a/F$ refer to this pocket. It is evident that the Weyl pocket produces the elongation $\Delta L/L$ that increases linearly with H at the high magnetic fields.

Consider the dependence of u_{zz} on the chemical potential ζ at a fix value of H (Supplementary Fig. 4). Since $F\propto S_{\max}\propto(\zeta-\varepsilon_d)^2$ and $n(\zeta-\varepsilon_d,0)\propto(\zeta-\varepsilon_d)^3$, we

arrive at

$$u_{zz} = \Lambda n(\zeta_0 - \varepsilon_d, 0)\frac{(\zeta-\varepsilon_d)^3}{(\zeta_0-\varepsilon_d)^3}\left(\frac{3B}{4F}\frac{(\zeta_0-\varepsilon_d)^2}{(\zeta-\varepsilon_d)^2}-1\right),$$

where ζ_0 is the initial value of the chemical potential. Supplementary figure 4 shows that the magnetostriction changes its sign when ζ crosses the energy of the Weyl point ε_d.

Weak magnetic fields ($\mu_0 H \ll F$). At $\mu_0 H \ll F$, the ratio u in Eq. (5) is large, and the sum contains many terms. Using the representation (7) and the expansion of the Hurwitz zeta function $\zeta(-1/2, u)$ at $u \gg 1$ [12],

$$\zeta(-1/2,u) \approx -\frac{2}{3}u^{3/2} + \frac{1}{2}u^{1/2} - \frac{1}{24u^{1/2}}, \qquad (11)$$

we find from formulas (2) and (5) that the magnetostriction u_{zz} produced by a Weyl pocket comprises the smooth and oscillating parts in the weak-field range, $u_{zz} = \bar{u}_{zz} + u_{zz}^{\rm osc}$. The smooth part $\bar{u}_{zz}$ has the form

$$\bar{u}_{zz} = \Lambda n(\zeta-\varepsilon_d,0)\frac{B^2}{16F^2} = -\frac{b^2}{9a}B^2 \equiv cB^2, \qquad (12)$$

and the oscillating part $u_{zz}^{\rm osc}$ results from the term $\zeta(-1/2, \{u\})$ in Eq. (7),

$$u_{zz}^{\rm osc} = \Lambda n(\zeta-\varepsilon_d,0)\frac{3\zeta(-1/2,\{u\})}{2u^{3/2}}. \qquad (13)$$

The oscillating behavior of $u_{zz}^{\rm osc}$ with changing $u = F/B$ becomes evident from the formula [12],

$$\zeta(-1/2,\{u\}) = \frac{1}{2\pi\sqrt{2}}\sum_{n=1}^{\infty}\frac{1}{n^{3/2}}\sin\left(2\pi n u - \frac{\pi}{4}\right). \qquad (14)$$

Interestingly, with changing the chemical potential, the coefficient c sharply changes it sign when ζ crosses the energy of the Weyl point (Supplementary Fig. 4),

$$c(\zeta) = c(\zeta_0)\frac{(\zeta_0-\varepsilon_d)}{(\zeta-\varepsilon_d)}, \qquad (15)$$

where ζ_0 is the initial value of ζ. Note that $c(\zeta)$ diverges at $\zeta = \varepsilon_d$.

Formulas (10), (12), (13), and (15) are written at $T = 0$. A nonzero temperature tends to suppress the oscillations of the magnetostriction, but it has effect on $\bar{u}_{zz}$ only in the region $|\zeta - \varepsilon_d| \lesssim T$. In this region, the divergence of $c(\zeta)$ near ε_d is cut off (Supplementary Fig. 4), and the maximal value of $c(\zeta)$ is of the order of $c(\zeta_0)(\zeta_0 - \varepsilon_d)/T$.

Finally, as an example, we calculate the magnetostriction produced by the two groups of the Weyl electrons (W1 and W2) and by the holes, assuming that the contribution of these holes to the magnetostriction can be described by the term $c_h B^2$ where c_h is a constant; see Supplementary Fig. 5. In this figure, the parameters c_h, a_{W1}, a_{W2}, F_{W1}, F_{W2}, and the dimensionless Dingle temperatures are found from the best fit of the calculated curve to the experimental data for TaAs presented in the main text.

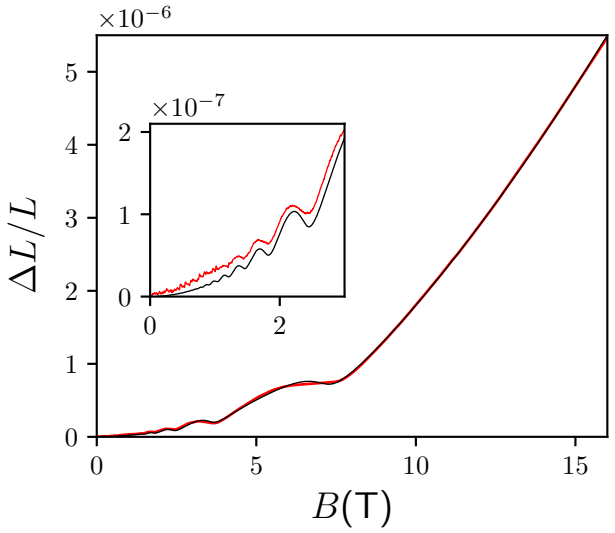

Supplementary Fig. 5. Comparison of the calculated magnetostriction with the experimental data for TaAs. The red line shows the c-axis magnetostriction $\Delta L/L$ of the crystal TaAs measured at $T = 25$ mK for the magnetic fields aligned with this axis, see Fig. 2(a) in the main text. The black line depicts the magnetostriction calculated at zero temperature, using equations (5) and (8) for the W1 and W2 electrons and assuming that $c_h B^2$ is the contribution of the holes to the magnetostriction. We use the following values of the parameters: $c_h = 1.49 \times 10^{-8}$ T^{-2}, $a_{W1} = -1.58 \times 10^{-6}$, $a_{W1} = -0.6 \times 10^{-6}$, $F_{W1} = 7.2$ T, $F_{W2} = 5$ T, $\gamma_{W1} = 0.025$ and $\pi T_{D,W2}/(\zeta - \varepsilon_{d,W2}) = 0.1$.

Supplementary Note 3: Magnetostriction produced by electrons with parabolic spectrum

For comparison, consider the magnetostriction u_{zz} produced by the "trivial" electrons with the parabolic dispersion,

$$\varepsilon(p_x,p_y,p_z) = \varepsilon_0 + \frac{p_x^2}{2m_x} + \frac{p_y^2}{2m_y} + \frac{p_z^2}{2m_z}, \qquad (16)$$

where ε_0 is the edge of the electron band, and m_x, m_y, m_z are the effective electron masses. In the magnetic field H these electrons have the well-known energy spectrum,

$$\varepsilon_n(p_\parallel) = \varepsilon_0 + \frac{eB\hbar}{m_*}(n+\frac{1}{2}+\delta) + \frac{p_\parallel^2}{2m_\parallel}, \qquad (17)$$

where n is an integer ($n \geq 0$); $p_\parallel$ is the quasi-momentum along the magnetic field; $m_\parallel$ and m_* are the longitudinal effective mass and the cyclotron mass, respectively, and the electron magnetic moment composed of its spin and orbital parts is written as $\delta(e\hbar/m_*)$, with δ being a constant. Since due to the time reversal symmetry, the contribution of any charge-carrier pocket to the Ω potential for a noncetrosymmetric crystal can be considered as a

half contribution of the same pocket with the states that are doubly degenerate in spin, one should imply that the parameter δ in the Zeeman term $\delta(e\hbar B/m_*)$ of Eq. (17) takes the values $+\delta$ and $-\delta$ (in this situation, δ can be represented in terms of the g factor, $\delta = gm_*/4m$). With this spectrum, we obtain at zero temperature,

$$n(\zeta-\varepsilon_0,B) = \frac{3n(\zeta-\varepsilon_0,0)}{4u^{3/2}} \sum_{\pm,n=0}^{n=[u-0.5\mp\delta]} \sqrt{u-\frac{1}{2}\mp\delta-n}, \quad (18)$$

where $n(\zeta-\varepsilon_0,B)$ is the density of the quasiparticles in the magnetic field $H = B/\mu_0$ at a given chemical potential ζ; the frequency F in the ratio $u \equiv F/B$ is still defined by formula (6). However, for the trivial electrons, the maximal cross sectional area $S_{\max}$ of their Fermi surface is proportional to $(\zeta-\varepsilon_0)$.

Ultra-quantum regime ($\mu_0 H > F$). At $\delta < 1/2$ and $\mu_0 H > B_{uq} = F/(0.5-\delta)$, the sum in equation (18) disappears. Then, with formula (2), we obtain the constant contribution of the trivial-electron pocket to the magnetostriction in this ultra-quantum limit,

$$u_{zz} = -\Lambda n(\zeta-\varepsilon_0,0) \equiv a. \quad (19)$$

Interestingly, at $\delta = 1/2$, this limiting value of u_{zz} cannot be reached since at any H, the lowest Landau subband remains occupied by the electrons. In this situation Eq. (18) reduces to formula (5) for the Weyl electrons.

When $\delta > 1/2$, the behavior of the magnetostriction in the ultra-quantum limit cardinally changes. It follows from Eq. (18) that

$$n(\zeta-\varepsilon_0,B) = \frac{3n(\zeta-\varepsilon_0,0)}{4u^{3/2}} \sqrt{u-\frac{1}{2}+\delta}, \quad (20)$$

$$n(\zeta-\varepsilon_0,B) = \frac{3n(\zeta-\varepsilon_0,0)}{4u^{3/2}} \left[\sqrt{u-\frac{1}{2}+\delta}+\sqrt{u-\frac{3}{2}+\delta}\right],$$

for $1/2 < \delta < 3/2$ at $\mu_0 H > F/(1.5-\delta)$ and for $3/2 < \delta < 5/2$ at $\mu_0 H > F/(2.5-\delta)$, respectively. In both the cases, $n(\zeta-\varepsilon_0,B) \propto B^{3/2}$ at $B \gg F$. The special case $\delta = 1/2$, for which the formula for the magnetostriction exactly coincides with the expression for the Weyl electron, separates the two essentially different behaviors of the magnetostriction in the ultra-quantum limit.

Weak magnetic fields ($\mu_0 H \ll F$). At $\mu_0 H \ll F$, the ratio u in Eq. (18) is large, and the sum contains many terms. Similarly to the case of the Weyl electrons, we find from formulas (2) and (18) that the magnetostriction u_{zz} produced by the trivial electrons comprises the smooth and oscillating parts in the weak-field range, $u_{zz} = \bar{u}_{zz} + u_{zz}^{\rm osc}$. These smooth ($\bar{u}_{zz}$) and oscillating ($u_{zz}^{\rm osc}$) parts have the following forms:

$$\bar{u}_{zz} = \Lambda n(\zeta-\varepsilon_0,0)\frac{3B^2}{8F^2}(\delta^2-\frac{1}{12}) \equiv cB^2, \quad (21)$$

$$u_{zz}^{\rm osc} = \frac{3\Lambda n(\zeta-\varepsilon_0,0)}{4u^{3/2}} \sum_{\pm} \zeta(-1/2,\{u-0.5\pm\delta\}), \quad (22)$$

where $\{x\} \equiv x-[x]$ is fractional part of x. Interestingly, at $\delta \to 0$ when the Zeeman energy is negligible as compared to the cyclotron spacing between the Landau subbands, we find that $c = -\Lambda n(\zeta-\varepsilon_0,0)/(32F^2)$. This value is of the opposite sign as compared to c for the Weyl electrons. On the other hand, the phase of the oscillating part (22) at $\delta \to 0$ is shifted by π with respect to the phase of the oscillations described by Eq. (13). This shift is caused by the difference in the Berry phases for these two cases [10, 14]. On the other hand, at $\delta = 1/2$ the constant c exactly coincides with that given by Eq. (12), and equation (22) for the oscillating part reduces to Eq. (13).

Thus, we find that the B-dependence of u_{zz} for the trivial electrons with $\delta \neq 1/2$ essentially differs from the appropriate dependence for the Weyl quasiparticles (see also Fig. 1 in the main text). This result enables one to distinguish between the Weyl and trivial electrons with measurements of the magnetic-field dependences of the magnetostriction. However, if $\delta = 1/2$, the formulas for the magnetostriction exactly coincide in these two cases.

According to Ref. [15, 16], the quantity δ is close to 1/2 for a band in a *centrosymmetric* crystal if this band is separated from another by a small gap that is less than the strength of the spin-orbit interaction. These bands are doubly degenerate in spin for such crystals. Strictly speaking, the spectrum (17) (with $\pm\delta$) is applicable to this situation only if the chemical potential measured from the edge of the band, $\zeta-\varepsilon_0$, is noticeably less than the gap Δ in the spectrum. However, it turns out that even if $\zeta-\varepsilon_0 \gtrsim \Delta$, the B dependence of the magnetostriction for the gapped spectrum coincides with its B dependence for Dirac electrons. In this context, it is worth noting that the spectrum of bismuth is sufficiently well described by a two-band model, the parameter δ is close to 1/2 [16], and so the field dependence of its magnetostriction [5, 17] is reminiscent of the appropriate dependence for the Dirac electrons. However, the situation essentially changes for the *noncentrosymmetric* Weyl semimetals considered here. In particular, the holes in TaAs are located near the nodal ring that would occur in this semimetal in neglect of the spin-orbit interaction [18]. The spin-orbit coupling lifts the degeneracy of the bands, and there are *four* close bands in the region of the Brillouin zone where the holes exist. In this situation, there is no reason to expect that $\delta \approx 1/2$ for them.

Finally, let us comment on the applicability of the rigid-band approximation, which has been used everywhere above. Consider the situation when a band of the trivial electrons is separated from a valence band by a sufficiently small gap Δ. In this case, the effective electron masses in Eq. (16) are of the order of Δ/V^2 where V is a typical interband matrix element of the velocity operator ($V \sim 10^5 \div 10^6$ m/s). If $\zeta-\varepsilon_0$ is not-too-small as compared to Δ, and not only ε_0 but also the gap Δ depend on a deformation, the rigid-band approximation can fail since the effective masses, and hence the shape

of the band, noticeably change with the deformation. In this case, formula (2) will contain an additional term, and in the weak-field range, this term is proportional to B^2.

Supplementary Note 4: Magnetostriction of TaAs

In Supplementary Notes 2 and 3 the B-dependences of the magnetostriction are analyzed under the assumption that a variation of the magnetic field does not change the chemical potential ζ of electrons. This situation does can occur when a crystal contains a large charge-carrier group that maintains the constancy of the chemical potential. However, in TaAs there are eight equivalent pockets of the W1 electrons, sixteen equivalent pockets of the W2 electrons, and eight equivalent pockets of the holes, with all the pockets being relatively small. In this case it is necessary to take into account the magnetic-field dependence of the chemical potential in analyzing the magnetostriction. This dependence $\zeta(B)$ is found from the conservation condition of the total density of the charge carriers,

$$\sum_i [n_i(\zeta, B) - n_i(\zeta_0, 0)] = 0, \tag{23}$$

where the summation is over all the pockets, ζ_0 is the initial value of ζ at $H = 0$, and the charge-carrier density in the magnetic field for the ith pocket, $n_i(\zeta, B)$, is described by formula (5) for the Weyl electrons and by Eq. (18) for the holes [or by some other expression if the spectrum of the holes differs from that given by Eq. (17)]. With the B-dependence of ζ, formula (2) is rewritten as follows:

$$u_{zz} = \sum_i^N \Lambda_i [n_i(\zeta, B) - n_i(\zeta_0, 0)]. \tag{24}$$

It is clear from Eqs. (23) and (24) that if all the constants Λ_i were the same, the magnetostriction u_{zz} would be zero.

Consider a special case when the magnetic field is considerably less than the fields F_i/μ_0 for all the groups of the charge carriers. In this situation, equation (23) in the chemical potential ζ is approximately solvable since the difference $n_i(\zeta, B) - n_i(\zeta_0, 0)$ can be rewritten as follows:

$$\begin{aligned} n_i(\zeta, B) - n_i(\zeta_0, 0) &= n_i(\zeta, B) - n_i(\zeta_0, B) \\ &+ n_i(\zeta_0, B) - n_i(\zeta_0, 0) \approx \nu_i(\zeta - \zeta_0) \\ &+ n_i(\zeta_0, B) - n_i(\zeta_0, 0), \end{aligned}$$

where $\nu_i \equiv \partial n_i(\zeta_0, 0)/\partial\zeta_0$, and we have taken into account that $\partial n_i(\zeta, B)/\partial\zeta \approx \nu_i$ at the weak magnetic fields $\mu_0 H \ll F_i$. Then, equations (23) and (24) give

$$\begin{aligned} (\zeta - \zeta_0) &= \frac{\sum_i [n_i(\zeta_0, B) - n_i(\zeta_0, 0)]}{\nu}, \\ u_{zz} &= \sum_i \tilde{\Lambda}_i [n_i(\zeta_0, B) - n_i(\zeta_0, 0)], \\ \tilde{\Lambda}_i &= \sum_m \frac{\nu_m}{\nu}(\Lambda_i - \Lambda_m), \end{aligned} \tag{25}$$

where $\nu \equiv \sum_i \nu_i$. Therefore, in this weak-field range the B-dependence of the chemical potential can be taken into account by the renormalization of the constants Λ_i. For stronger magnetic fields, it is necessary to solve equation (23) numerically.

In the case of TaAs, it is convenient to rewrite general formula (24) with the use of Eq. (23) as follows:

$$\begin{aligned} u_{zz} = (\Lambda_{W1} - \Lambda_h) \sum_{i=1}^{8} [n_i(\zeta, B) - n_i(\zeta_0, 0)] \\ + (\Lambda_{W2} - \Lambda_h) \sum_{i=1}^{16} [n_i(\zeta, B) - n_i(\zeta_0, 0)], \end{aligned} \tag{26}$$

where the summation is carried out over the W1 and W2 pockets only; the constants Λ_{W1}, Λ_{W2}, and Λ_h refer to the W1, W2 electrons, and to the holes, respectively. This formula is valid at any strength of the magnetic fields. In the weak magnetic fields, $\mu_0 H \ll F_i$, formulas (23) and (26) are equivalent to Eqs. (25).

Magnetic field parallel to the c axis. When the magnetic field is parallel to the c axis, all the pockets in the W1 electron group or in the W2 group or in the hole group give identical contributions to the magnetostriction. Let F_{W1}, F_{W2}, and F_h denote the frequencies F_i for the W1 and W2 electrons pockets and for the holes, respectively. According to Ref. [18], at this direction of H one has $F_{W1} \sim 7$ T, $F_{W2} \sim 5$ T, and the field $F_h \sim 19$ T for the holes is larger than the maximal field 16 T in our experiments. Since F_h is large, we shall consider the range $\mu_0 H \leq 16$ T as the low-field region for the holes and shall describe their contribution to Eq. (23) as follows:

$$\begin{aligned} n_h(\zeta, B) - n_h(\zeta_0, 0) &= n_h(\zeta, B) - n_h(\zeta, 0) \\ &+ n_h(\zeta, 0) - n_h(\zeta_0, 0) \\ &\approx B^2 \Big(\beta(\zeta_0) + \frac{d\beta(\zeta_0)}{d\zeta_0}(\zeta - \zeta_0) \Big) + \nu_h(\zeta_0)(\zeta - \zeta_0), \end{aligned} \tag{27}$$

where $\nu_h = \partial n_h(\zeta, 0)/\partial\zeta$ is density of states for the holes in zero magnetic field, whereas the function $\beta(\zeta)$ defines the variation of the hole density for the low magnetic fields,

$$n_h(\zeta, B) - n_h(\zeta, 0) = \beta(\zeta) B^2.$$

(The oscillation contribution to $n_h(\zeta, B)$ is neglected.) If the holes can be described by the parabolic spectrum

(16), (17), one arrives at [compare with Eq. (21)],

$$\beta(\zeta)=\frac{3n_h(\zeta,0)}{8F_h^2}(\delta^2-\frac{1}{12}),\\ \frac{d\beta(\zeta)}{d\zeta}=\frac{\beta(\zeta)}{2(\varepsilon_0-\zeta)},\\ \nu_h(\zeta)=-\frac{3n_h(\zeta,0)}{2(\varepsilon_0-\zeta)}, \tag{28}$$

where ε_0 is the edge of the hole band, and we have taken into account that $n_h(\zeta,0)\propto(\varepsilon_0-\zeta)^{3/2}$ and $n_h(\zeta,0)/F_h^2(\zeta)\propto(\varepsilon_0-\zeta)^{-1/2}$ for the parabolic spectrum. However, we emphasize that formula (27) is applicable to the holes even though their spectrum is not described by the parabolic model, and their Fermi surface noticeably differs from an ellipsoid. The only requirement of the applicability is the condition of the low-field limit for them (i.e., $B<F_h$).

Let us introduce the dimensionless deviation of the chemical potential from its initial value at $H=0$, $\delta\tilde{\zeta}\equiv(\zeta-\zeta_0)/(\zeta_0-\varepsilon_{d,W1})$ where $\varepsilon_{d,W1}$ is the energy of the Weyl points W1. Then, at $T=0$, equation (23) that determines $\delta\tilde{\zeta}(B)$ is rewritten as follows:

$$\left(1-\frac{3(1+\delta\tilde{\zeta})}{4u_1}-\frac{3}{2u_1^{3/2}}\sum_{n=1}^{n=[u_1]}\sqrt{u_1(1+\delta\tilde{\zeta})^2-n}\right)\\ +\frac{n_{W2}}{n_{W1}}\left(1-\frac{3(1+v\delta\tilde{\zeta})}{4u_2}-\frac{3}{2u_2^{3/2}}\sum_{n=1}^{n=[u_2]}\sqrt{u_2(1+v\delta\tilde{\zeta})^2-n}\right)\\ -B^2(\tilde{\beta}_0+\tilde{\beta}_1\delta\tilde{\zeta})-\tilde{\nu}_h\delta\tilde{\zeta}=0, \tag{29}$$

where n_{W1}, n_{W2} are the densities of the electrons at zero magnetic field (i.e., at $\zeta=\zeta_0$); $v\equiv(\zeta_0-\varepsilon_{d,W1})/(\zeta_0-\varepsilon_{d,W2})$; $\varepsilon_{d,W2}$ is the energy of the Weyl points W2,

$$\tilde{\beta}_0\equiv-\frac{\beta(\zeta_0)}{n_{W1}},\\ \tilde{\beta}_1\equiv-\frac{(\zeta_0-\varepsilon_{d,W1})}{n_{W1}}\frac{d\beta(\zeta_0)}{d\zeta_0},\\ \tilde{\nu}_h\equiv-\frac{(\zeta_0-\varepsilon_{d,W1})}{n_{W1}}\nu_h(\zeta_0);$$

$u_1=F_{W1}/B$, $u_2=F_{W2}/B$, and the frequencies F_{W1}, F_{W2} are taken at $\zeta=\zeta_0$. The densities n_i satisfies the relation $n_{W1}+n_{W2}-|n_h|=n_{\rm imp}$ where n_h is the hole density at $H=0$, and the charge carrier density $n_{\rm imp}$ is caused by impurities. This $n_{\rm imp}$ specifies the doping in the sample. With the doping, $1+(n_{W2}/n_{W1})-(|n_h|/n_{W1})\neq 0$.

In the case of the parabolic spectrum for the holes, we obtain from Eqs. (28),

$$\tilde{\beta}_0=\frac{3|n_h|}{(8F_h^2n_{W1})}(\delta^2-\frac{1}{12}),\\ \frac{\tilde{\beta}_1}{\tilde{\beta}_0}=\frac{(\zeta_0-\varepsilon_{d,W1})}{2(\varepsilon_0-\zeta_0)},\\ \tilde{\nu}_h=-\frac{3|n_h|(\zeta_0-\varepsilon_{d,W1})}{2n_{W1}(\varepsilon_0-\zeta_0)}=-\frac{3|n_h|}{n_{W1}}\frac{\tilde{\beta}_1}{\tilde{\beta}_0}.$$

Interestingly, if the magnetic field is tilted away from the c axis, the quantities F_h, δ, and hence $\tilde{\beta}_0$, will change, but the ratio $\tilde{\beta}_1/\tilde{\beta}_0$ will remain unchanged for the parabolic spectrum. Of course, the parameters $\tilde{\nu}_h$, $\tilde{\beta}_0$, and $\tilde{\beta}_1$ may essentially differ from these estimates if the dispersion of the holes noticeably deviates from the parabolic law. As an example, let us consider a model situation when the dispersion of the holes is linear along the y and z directions in the Brillouin zone and is quadratic along the x axis. The real dispersion of the holes may be close to this model since the hole pockets are associated with the band-contact lines that would occur in TaAs in absence of the spin-orbit interaction [18]. Within this model, $n_h\propto(\varepsilon_0-\zeta_0)^{5/2}$, and $F_h\propto(\varepsilon_0-\zeta_0)^{3/2}$ when H is aligned with the z axis, whereas $F_h\propto(\varepsilon_0-\zeta_0)^2$ if H is directed along the x axis. If β in the first case ($H\parallel z$) is still proportional to $n_h(\zeta,0)/F_h^2$, the ratio $\tilde{\beta}_1/\tilde{\beta}_0$ remains the same as for the parabolic dispersion, but in the second case ($H\parallel x$), this ratio is equal to $(3/2)(\zeta_0-\varepsilon_{d,W1})/(\varepsilon_0-\zeta_0)$, i.e., it increases by the factor 3. Therefore, a deviation of the magnetic field from the z axis seems to cause a change of $\tilde{\beta}_1/\tilde{\beta}_0$ for such a model, and this ratio may sharply increase with the tilt angle if the elongation of the hole Fermi surface is sufficiently large in the x direction.

According to expression (26), the general formula for the magnetostriction $\Delta L/L=u_{zz}$ of TaAs at zero temperature takes the form:

$$\frac{\Delta L}{L}=A_{W1}\Big(1-\frac{3(1+\delta\tilde{\zeta})}{4u_1}\\ -\frac{3}{2u_1^{3/2}}\sum_{n=1}^{n=[u_1]}\sqrt{u_1(1+\delta\tilde{\zeta})^2-n}\Big)+A_{W2}\Big(1-\frac{3(1+v\delta\tilde{\zeta})}{4u_2}\\ -\frac{3}{2u_2^{3/2}}\sum_{n=1}^{n=[u_2]}\sqrt{u_2(1+v\delta\tilde{\zeta})^2-n}\Big), \tag{30}$$

where $A_{W1}\equiv-(\Lambda_{1,W1}-\Lambda_{1,h})n_{W1}$, $A_{W2}\equiv-(\Lambda_{1,W2}-\Lambda_{1,h})n_{W2}$, and $\delta\tilde{\zeta}(H)$ is found from Eq. (29).

To take into account the electron scattering by impurities, we use the representation (8) for the sums in Eqs. (29) and (30) and replace ζ by $\zeta+i\Gamma_i$ where the quantity Γ_i characterizes the scattering of charge carriers in the pocket i ($i=$W1, W2); see the Supplementary Note 2. This means that $\delta\tilde{\zeta}$ is replaced by $\delta\tilde{\zeta}+i\gamma_{W1}$ or $\delta\tilde{\zeta}+i\gamma_{W2}$ in the appropriate terms of Eqs. (29) and (30) where $\gamma_i=\Gamma_i/(\zeta-\varepsilon_{W1})$.

The magnetostriction at nonzero temperature can be calculated with formula (9). In order to apply this formula, let us introduce the new variable $x \equiv (\varepsilon-\zeta)/(\zeta_0-\varepsilon_{d,W1})$ in integral (9) and the dimensionless temperature $t \equiv T/(\zeta_0-\varepsilon_{d,W1})$. Then, Eq. (9) is rearranged as follows:

$$u_{zz}(\zeta,T)=\frac{1}{4t}\int_{-\infty}^{\infty}dx\frac{u_{zz}(x,0)}{\cosh^2(x/2t)}, \qquad (31)$$

where $u_{zz}(x,0)$ is given by formula (30) in which the factors $(1+\delta\tilde{\zeta})$ and $(1+v\delta\tilde{\zeta})$ are replaced by $(1+\delta\tilde{\zeta}+x)$ and $(1+v\delta\tilde{\zeta}+vx)$, respectively.

Supplementary Note 5: Estimates of the parameters for TaAs

It was demonstrated in Ref. [19] how one can estimate parameters characterizing Weyl Fermi pockets, using the data for the quantum-oscillation frequencies and for the appropriate cyclotron masses. In particular, if the frequency F produced by a Weyl pocket and the appropriate cyclotron mass m_* have been measured at least for one direction of the magnetic field, the formula

$$|\zeta-\varepsilon_d|=\frac{S_{\max}}{\pi|m_*|}=\frac{2e\hbar F}{|m_*|}, \qquad (32)$$

enables one to find the position of the chemical potential ζ relative to the energy ε_d of the Weyl point. Here $S_{\max}$ is the area of the extremal cross section perpendicular to the magnetic field for the Weyl pocket. The density n_W of the Weyl charge carriers can be expressed in terms of directly-measurable frequencies of the quantum oscillations,

$$n_W=\frac{N_W V}{(2\pi\hbar)^3}, \qquad (33)$$

where V is the volume of a Weyl pocket in the Brillouin zone,

$$V=\frac{4[S^{(1)}_{\max}S^{(2)}_{\max}S^{(3)}_{\max}]^{1/2}}{3\pi^{1/2}}=\frac{8\sqrt{2}\pi(e\hbar)^{3/2}(F_1F_2F_3)^{1/2}}{3} \qquad (34)$$

N_W is the numbers of the equivalent Weyl pockets, and F_i are the frequencies associated with the principal directions of the Fermi-surface ellipsoid. In other words, F_1 and F_3 are the maximal and minimal frequencies produced by the pocket when the magnetic field rotates in various planes, and F_2 corresponds to the direction of $\mathbf{H}$ perpendicular to the directions at which F_1 and F_2 occur. The cross sectional areas $S^{(i)}_{\max}$ correspond to the frequencies F_i, and these cross sections are mutually orthogonal.

In the case of the parabolic dispersion of charge carriers, the formula that is similar to Eq. (32) looks as follows:

$$|\zeta-\varepsilon_d|=\frac{S_{\max}}{2\pi|m_*|}=\frac{e\hbar F}{|m_*|}, \qquad (35)$$

and contains the additional factor 1/2 as compared to Eq. (32).

Using the experimental data for the cross-sectional areas and the cyclotron masses (Table I in Ref. [18]) and the calculated value $F_{W2}\sim 5$ T for H parallel to the c axis [18], we obtain with formulas (32)-(34) that $n_{W1}\approx 2.5\times10^{18}$ cm^3, $\zeta_0-\varepsilon_{d,W1}\approx 28.4\pm3.5$ meV [19], and $n_{W2}/n_{W1}\sim 0.15$, $\zeta_0-\varepsilon_{d,W2}\approx 11.9\pm1$ meV. In the case of the parabolic spectrum for the holes, we similarly can find $\varepsilon_0-\zeta_0$ using Eq. (35) and values of F and m_* measured for the hole at two directions of H [18]. It turns that $\varepsilon_0-\zeta_0$ lies in the interval 12.6–20.6 meV if the data for H parallel to [100] is used in the calculation, and $\varepsilon_0-\zeta_0$ is in the range 7.9–16.2 meV if we take the data for H parallel to the directions [110]. Therefore, it is reasonable to assume that 12.6 meV $<\varepsilon_0-\zeta_0<$ 16.2 meV. With these $\zeta_0-\varepsilon_{d,W1}$ and $\varepsilon_0-\zeta_0$, we arrive at the estimate,

$$\frac{\tilde{\beta}_1}{\tilde{\beta}_0}=\frac{(\zeta_0-\varepsilon_{d,W1})}{2(\varepsilon_0-\zeta_0)}\approx 0.8\div1.3.$$

If the dispersion of the hole is quadratic in the [100] direction and is linear in the (100) plane (see Supplementary Note 4), formula (32) is more appropriate for the estimates of $\varepsilon_0-\zeta_0$ from the data of Ref. [18], and we obtain approximately a twofold increase in $\varepsilon_0-\zeta_0$, and hence $\tilde{\beta}_1/\tilde{\beta}_0$ decreases by the factor ~ 2.

Since the oscillations in the magnetostriction of our sample and the quantum oscillations observed by Arnold et al. [18] for the W1 electrons have practically the same frequency at H parallel to the c axis, we conclude that the Fermi-surface parameters estimated above are appropriate for our samples, too. However, it is necessary to emphasize that the experimental c-axis magnetostriction can be well fitted by the theoretical curve calculated with the equations of Supplementary Note 4 even if the Fermi-surface parameters differ from those evaluated above (Supplementary Fig. 6).

Supplementary Note 6: Dependence of the magnetostriction on the magnetic-field direction

When the magnetic field is tilted away from the c axis in the plane (010), electron pockets in the W1, W2 groups, as well as the hole pockets, produce different contributions to the magnetostriction, and one should take into account that with increasing the tilt, the parameters F_{W1}, F_{W2}, F_h not only change in magnitude but also the number of these parameters increases (the charge-carrier pockets in any group have different values of these parameters). This makes the strict theoretical analysis of the magnetostriction very complicated. Here we carry out an approximate calculation of the c-axis magnetostriction when the magnetic field is tilted away from the c axis at a not-too-large angle $\theta=25°$, assuming that at

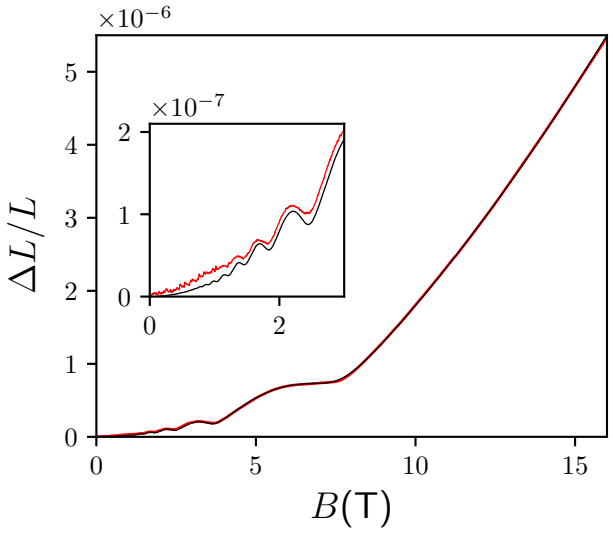

Supplementary Fig. 6. Comparison of the calculated magnetostriction with the experimental data for TaAs. The red line shows the c-axis magnetostriction $\Delta L/L$ of the crystal TaAs measured at $T = 25$ mK and $H \parallel c$, see Fig. 2(a) in the main text. The black line depicts the magnetostriction calculated with equations (29), (30) of Supplementary Note 4 at zero temperature and at the values of the parameters presented in Table I of the main text (set No. 2).

this angle, the frequencies $F_h(\theta)$ for different hole pockets continue to exceed 16 T. In this situation (at $B < 16$ T), we still can describe the holes density with formula (27). For simplicity, we shall also assume that the Fermi-surface of the W2 electrons is close to a sphere, i.e., the dispersion of these charge carriers is almost isotropic. In this case, the frequency F_{W2} is practically independent of θ, and we set $F_{W2}(\theta) = 5$ T. As to the W1 electrons, their pockets located near the a and b axes of the TaAs crystal generally produce different oscillation frequencies $F_{W1}(\theta)$ that are described by the following expressions [19]:

$$\frac{F_{W1}(\theta)}{F_{W1}(0)} \approx \frac{1}{\sqrt{\cos^2\theta + 0.058\sin^2\theta}}, \qquad (36)$$

$$\frac{F_{W1}(\theta)}{F_{W1}(0)} \approx \frac{1}{\sqrt{\cos^2\theta + 0.014\sin^2\theta}}, \qquad (37)$$

where we have used the values of parameters found in Ref. [19], and $F_{W1}(0)$ is the frequency at H aligned with the c axis. For $F_{W1}(0) = 7.2$ T, these two branches of $F_{W1}(\theta)$ give the following two frequencies: $F_{W1}(25°) \approx 7.89$ T and $F_{W1}(25°) \approx 7.93$ T. Since these values are close to each other, we shall set below that all the W1 pockets produce the same frequency $F_{W1}(25°) = 7.9$ T.

As follows from the definitions of A_{W1}, A_{W2}, an $\tilde{\nu}_h$, a tilt of the magnetic field from the c axis does not change these parameters, and we take the same values

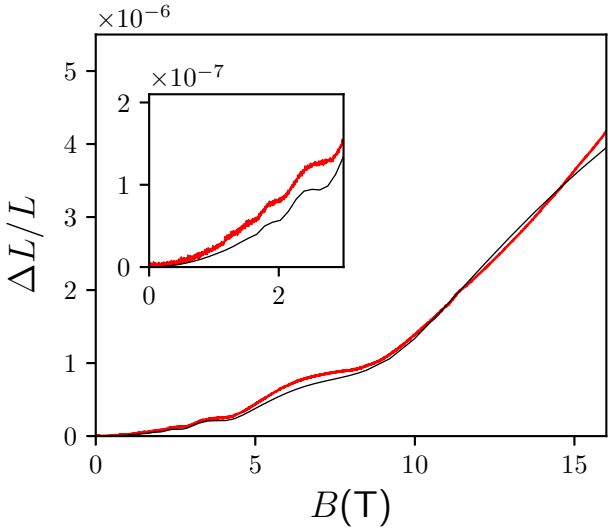

Supplementary Fig. 7. Comparison of the calculated magnetostriction with the experimental data for TaAs. The red line shows the c-axis magnetostriction $\Delta L/L$ of the crystal TaAs measured at $T = 4.2$ K for the magnetic field directed at the angle $\theta = 25°$ to the c axis (see Fig. 7 in the main text). The black line depicts the magnetostriction calculated with equations (29)–(31) of Supplementary Note 4 for $t = 0.015$ and at the values of the parameters presented in Table I of the main text (set No. 1), but with changed $\tilde{\beta}_0 \approx 1.30 \times 10^{-3}$ T^{-2}, $\tilde{\beta}_1 \approx 2.91 \times 10^{-3}$ T^{-2}.

of them as in Table I of the main text (set No. 1): $A_{W1} = -10.9 \times 10^{-6}$, $A_{W1} = -1.92 \times 10^{-6}$, $\tilde{\nu}_h = -0.91$. However, the parameters $\tilde{\beta}_0$ and $\tilde{\beta}_1$ may depend on θ, and we find them from the best fit of the calculated B-dependence of the magnetostriction to the experimental data (Supplementary Fig. 7): $\tilde{\beta}_0 \approx 1.30 \times 10^{-3}$ T^{-2}, $\tilde{\beta}_1 \approx 2.91 \times 10^{-3}$ T^{-2}. Note that the ratio $\tilde{\beta}_1/\tilde{\beta}_0$ is essentially increases as compared to the case of $\theta = 0$ (Table I in the main text). According to the Supplementary Note 4, this result seems to indicate that the dispersion of the holes in TaAs is not described by a simple parabolic law. In other words, the conventional holes in TaAs (the spectrum of which does not contain the Weyl nodes) probably cannot be considered as the trivial charge carriers described by a simple parabolic dispersion.

[1] Küchler, R., Bauer, T., Brando, M. & Steglich, F. A compact and miniaturized high resolution capacitance dilatometer for measuring thermal expansion and magnetostriction. *Rev. Sci. Instrum.* **83**, 095102 (2012).

[2] Landau, L.D. & Lifshitz, E.M. *Theory of Elasticity* (Pergamon Press, 1981).

[3] Mikitik, G.P. Sharlai, Yu.V. Specific features of magnetostriction at electron topological transitions in metals. *Fiz. Nizk. Temp.* **43**, 200 (2017) [*Low Temp. Phys.* **43**, 168 (2017)].

[4] Keyes, R. W. Electronic Effects in the Elastic Properties of Semiconductors. *Solid State Phys.* **20**, 37 (1968).

[5] Michenaud, J-P., Heremans, J., Shayegan, M. & Haumont, C. Magnetostriction of bismuth in quantizing magnetic fields. *Phys. Rev. B* **26**, 2552-2559 (1982).

[6] Mikitik, G. P. & Sharlai, Yu. V. Magnetic susceptibility of topological nodal semimetals. *Phys. Rev. B* **94**, 195123 (2016).

[7] dos Reis, R. D. et al. On the search for the chiral anomaly in Weyl semimetals: the negative longitudinal magnetoresistance. *N. J. Phys.* **18**, 085006 (2016).

[8] Abrikosov, A.A. *Fundumentals of the theory of metals* (North-Holland, Amsterdam, 1988).

[9] Buckeridge, J., Jevdokimovs, D., Catlow, C.R.A. & Sokol, A.A. *Phys. Rev. B* **93**, 125205 (2016).

[10] Mikitik, G. P. & Sharlai, Yu. V. Magnetic Susceptibility of Topological Semimetals. *J. Low Temp. Phys.* **197**, 272 (2019).

[11] Mikitik, G.P. & Sharlai, Yu. V. Field dependences of magnetic susceptibility of crystals under conditions of degeneracy of their electron energy bands. *Fiz. Nizk. Temp.* **22**, 762 (1996) [*Low Temp. Phys.* **22**, 585 (1996)].

[12] Bateman, H. & Erdelyi, A. *Higher transcendental functions Vol. 1, Ch. 1.10 and 1.18* (Mc Graw-Hill Book Company, Inc, New York, Toronto, London, 1953).

[13] Shoenberg, D. *Magnetic Oscillations in Metals* (Cambridge University Press, Cambridge, England, 1984).

[14] Mikitik, G. P. & Sharlai, Yu. V. Manifestation of Berry's phase in metal physics. *Phys. Rev. Lett.* **82**, 2147-2150 (1999).

[15] Mikitik, G. P. & Sharlai, Yu. V. g factor of conduction electrons in the de Haas−van Alphen effect. *Phys. Rev. B* **65**, 184426 (2002).

[16] Mikitik, G. P. & Sharlai, Yu. V. Calculation of conduction electron g factor in metals: Comparison of electron-spin dynamics and local g-factor approaches. *Phys. Rev. B* **67**, 115114 (2003).

[17] Küchler, R. et al. Thermodynamic evidence for valley-dependent density of states in bulk bismuth. *Nat. Mater.* **13**, 461-465 (2014).

[18] Arnold, F. et al. Chiral Weyl pockets and Fermi surface topology of the Weyl semimetal TaAs. *Phys. Rev. Lett.* **117**, 146401 (2016).

[19] Mikitik, G. P. & Sharlai, Yu. V. Analysis of Dirac and Weyl points in topological semimetals via oscillation effects. *Fiz. Nizk. Temp.* **47**, 342 (2021) [*Low Temp. Phys.* **47**, 312-317 (2021)].